INDIAN JOURNAL OF SCIENCE AND TECHNOLOGY

RESEARCH ARTICLE

Electrically conducting fluid flow with Nanoparticles in an inclined tapering Stenoses Artery through porous medium

K Maruthi Prasad[1], Prabhaker Reddy Yasa[2]*

1 Department of Mathematics, School of Science, GITAM (Deemed to be University), Hyderabad, 502 329, Telangana, India
2 Department of BS&H, B V Raju Institute of Technology (BVRIT), Narsapur, 502 313, Telangana, India. Tel.: +91-996-315-9601

OPEN ACCESS

Received: 30.11.2020
Accepted: 22.12.2020
Published: 04.01.2021

Citation: Maruthi Prasad K, Yasa PR (2020) Electrically conducting fluid flow with Nanoparticles in an inclined tapering Stenoses Artery through porous medium. Indian Journal of Science and Technology 13(48): 4708-4722. https://doi.org/10.17485/IJST/v13i48.2162

* **Corresponding author**.

Tel: +91-996-315-9601
prabhakerreddy.yasa@gmail.com

Funding: None

Competing Interests: None

Published By Indian Society for Education and Environment (iSee)

ISSN
Print: 0974-6846
Electronic: 0974-5645

Abstract

Objectives: A Mathematical Model is built in an inclined tapered artery having permeable walls for a blood flow with nanoparticles through porous media. **Methods/Statistical analysis**: The Nanoparticle phenomena and Temperature profiles are determined using Homotopy Perturbation Method (HPM). **Findings**: Analysis on resistance (or) Impedance to the flow and shear stress distribution in the stenotic area with regard to different flow parameters with stenosis height has been estimated by deriving the flow characteristic expressions and the solutions obtained. For various flow parameters, the variations of flow resistance as well as shear stress with stenosis height are illustrated graphically. For study of the fluid flow properties, streamline patterns are also drawn. It is remarkable to take note that, in converging $(\xi < 0)$, non-tapered $(\xi = 0)$ and diverging regions $(\xi > 0)$, the flow patterns are significantly impacted by magnetic field existence.

Keywords: Porous medium; tapered artery; Stenosis; Nanofluid; magnetic parameter

1 Introduction

The investigation of fluid flow through tubes with a permeable wall have many applications in biological as well as engineering systems. The role of human cardiovascular system is to deliver blood to nerves with optimal pressure to move materials across blood vessels. In cardiovascular related issues, the effected arteries get solidified because of accumulation of fatty materials. The substances stored in the arteries is called stenosis. The well-known valvular heart diseases in the world's developed and developing nations is Stenosis. Vascular fluid dynamics play a substantial job in enhancing vascular stenosis, which is among the most problematic diseases in humans that leads to cardiovascular system failure. The movement of the fluid gets interrupted, depending on the severity of the stenosis. Hence, the mathematical modelling of these type of flows may help to better understand and prevent arterial diseases.

Many researchers have done their work by considering the state of vessel's no-slip boundary at walls. Yet, physiological systems, the walls are in general permeable. Many investigators previously stated that the blood stream is Newtonian. Argument of this Newtonian blood conduct is reasonable for high viscosity rate stream. Blood has Non-Newtonian properties in certain cases [1–4].

The study of nanofluid particles is attracted by many researchers. [5], firstly introduced the concept of nanofluid. The non-Newtonian fluids with nano particles have attained much interest by many researchers [6].

Number of research studies theoretically investigated the flow of blood across permeable walls. [7] studied in detail the movement of fluid into an artery with permeable wall. The nano fluid movement in tapering stenosis arteries having permeable surfaces has been explored by [8].

Many researchers have surveyed different scientific models to examine fluid behaviour in the magnetic field existence. Investigators such as [9] studied fluid flow through porous media. [10] analysed the flow of nanofluid and heat transfer into porous media.

In [11] investigated the magneto-hydrodynamic impacts on blood flows into porous media. [12] evaluated the peristaltic transport of porous bounding magneto fluid. [13] delivered an abnormal study of the non-Newtonian fluid flow into tapering arteries, having stenosis. It introduces electric and magnetic fields whenever we impose magnetic field to a traveling electrically conductive fluid. For fluid supply in arteries, disorders such as stenosis, the role of magnetic field is used as a fluid pump in cardiac treatments. Likewise, impact of vessels formed by stenosis on the character of the flow seems incredibly significant. The impact of magnetic field on supply of blood across arteries was studied by [14]. [15] has researched slip impacts on unstable MHD pulsatile fluid movement across porous media in the artery, over body acceleration effect.

In this study, the influence of nanofluid flow characteristics under magnetic effect in an inclined tapering porous media has been examined. Pressure drop, Flow resistance and the Shear stress expressions are obtained. Impact of individual fluid parameters on fluid flow variables were discussed through the graphs. Fluid streamline patterns were discussed.

2 Mathematical Formulation

A polar coordinate system (r, θ, z) is considered and z-axis is along tube axis. An incompressible stream of nanofluid into an inclined tapering artery having stenosis with fluid viscosity μ and density ρ is considered. The radial and circumferential direction be r, θ respectively.

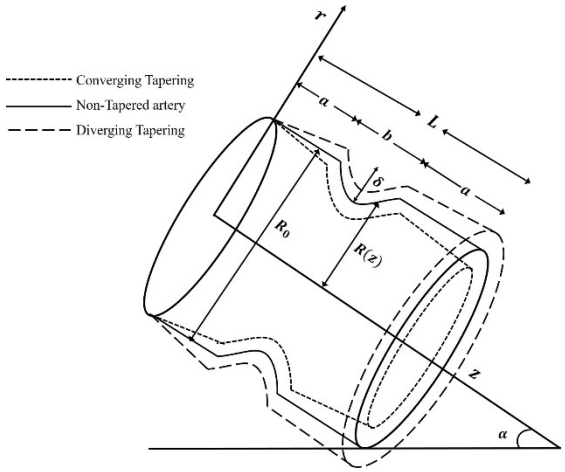

Fig 1. Geometry representation of inclined stenosed tapering artery

Assume that, stenoses form in an axially symmetric direction. The cylindrical tubular radius is taken as

$$h = R(z) = \begin{cases} f(z)\left[1 - \eta\left(b^{n-1}(z-a) - (z-a)^n\right)\right]; a \le z \le a+b \\ f(z); \text{ Otherwise} \end{cases} \quad (1)$$

Here, $f(z)$ and R_0 are respectively radius of tapering arterial segment in stenotic area and non-tapering artery in non-stenotic area, where $f(z) = R_0 + \xi z$, ξ is tapering parameter, $n(\geq 2)$ is shape parameter that defines stenosis shape, b is stenosis length.

$\eta = \frac{\delta}{R_0 b^n}\left(\frac{n^{\frac{1}{(n-1)}}}{n-1}\right)$ is a parameter, δ being the maximum height of stenosis at $z = a + \frac{b}{n^{\left(\frac{1}{n-1}\right)}}$.

Governing equations are given by[8]

$$\frac{1}{\bar{r}}\frac{\partial\left(\bar{r}\bar{v}\right)}{\partial\bar{r}} + \frac{\partial\bar{w}}{\partial\bar{z}} = 0 \tag{2}$$

$$\rho\left[\bar{v}\frac{\partial\bar{v}}{\partial\bar{r}} + \bar{u}\frac{\partial\bar{v}}{\partial\bar{z}}\right] = -\frac{\partial\bar{p}}{\partial\bar{r}} + \mu\left[\frac{\partial^2\bar{v}}{\partial\bar{r}^2} + \frac{1}{\bar{r}}\frac{\partial\bar{v}}{\partial\bar{r}} + \frac{\partial^2\bar{v}}{\partial\bar{z}^2} - \frac{\bar{v}}{\bar{r}^2}\right] - \frac{\cos\alpha}{F} \tag{3}$$

$$\rho\left[\bar{v}\frac{\partial\bar{u}}{\partial\bar{r}} + \bar{w}\frac{\partial\bar{u}}{\partial\bar{z}}\right] = -\frac{\partial\bar{p}}{\partial\bar{z}} + \mu\left[\frac{\partial^2\bar{w}}{\partial\bar{r}^2} + \frac{1}{\bar{r}}\frac{\partial\bar{w}}{\partial\bar{r}} + \frac{\partial^2\bar{w}}{\partial\bar{z}^2}\right] + \rho g\alpha\left(\bar{T} - \bar{T}_0\right) + \rho g\alpha\left(\bar{C} - \bar{C}_0\right) + \frac{\sin\alpha}{F} - \frac{\mu\bar{w}}{k} + \bar{J}\times\bar{B}, \tag{4}$$

$$\left[\bar{v}\frac{\partial\bar{T}}{\partial\bar{r}} + \bar{w}\frac{\partial\bar{T}}{\partial\bar{z}}\right] = \alpha\left[\frac{\partial^2\bar{T}}{\partial\bar{r}^2} + \frac{1}{\bar{r}}\frac{\partial\bar{T}}{\partial\bar{r}} + \frac{\partial^2\bar{T}}{\partial\bar{z}^2}\right] + \tau\left\{D_B\left[\frac{\partial\bar{C}}{\partial\bar{r}}\frac{\partial\bar{T}}{\partial\bar{r}} + \frac{\partial\bar{C}}{\partial\bar{z}}\frac{\partial\bar{T}}{\partial\bar{z}}\right] + \frac{D_{\bar{T}}}{\bar{T}_0}\left[\left(\frac{\partial\bar{T}}{\partial\bar{r}}\right)^2 + \left(\frac{\partial\bar{T}}{\partial\bar{z}}\right)^2\right]\right\} \tag{5}$$

$$\left[\bar{v}\frac{\partial\bar{C}}{\partial\bar{r}} + \bar{W}\frac{\partial C}{\partial\bar{z}}\right] = D_B\left[\frac{\partial^2\bar{C}}{\partial\bar{r}^2} + \frac{1}{\bar{r}}\frac{\partial\bar{C}}{\partial\bar{r}} + \frac{\partial^2\bar{C}}{\partial\bar{z}^2}\right] + \frac{D_{\bar{T}}}{\bar{T}_0}\left[\frac{\partial^2\bar{T}}{\partial\bar{r}^2} + \frac{1}{\bar{r}}\frac{\partial\bar{T}}{\partial\bar{r}} + \frac{\partial^2\bar{T}}{\partial\bar{z}^2}\right] \tag{6}$$

where $\tau = \frac{(\rho C)_P}{(\rho C)_f}$ is ratio to nano particle's effective heat capacity and the fluid's heat capacity. Here, $\bar{P}$ is pressure, $\bar{C}$ is nanoparticle phenomena, $D_{\bar{T}, D_B}$ being thermophoretic and Brownian diffusion coefficient respectively.

Boundary conditions are

$$\frac{\partial\bar{w}}{\partial\bar{r}} = 0,\ \frac{\partial\bar{T}}{\partial\bar{r}} = 0,\ \frac{\partial\bar{C}}{\partial\bar{r}} = 0\ at\ \bar{r} = 0 \tag{7}$$

$$\bar{w} = -k\frac{\partial\bar{w}}{\partial r}\ ,\ \bar{T} = \bar{T}_0\ ,\ \bar{C} = \bar{C}_0\ at\ \bar{r} = R(z) \tag{8}$$

Introducing the Non-dimensional quantities

$$\begin{aligned}
&\bar{z} = \frac{z}{B}, \bar{w} = \frac{w}{W}, \bar{v} = \frac{B}{\delta W}v, \bar{R}(z) = \frac{R(z)}{R_0}, \bar{\delta}_i = \frac{\delta_i}{R_0}, \bar{P} = \frac{P}{\mu W\ L/R_0^2}, \bar{q} = \frac{q}{\pi R_0^2 W}, R_e = \frac{2\rho c_1 R_0}{\mu}\\
&N_b = \frac{(\rho C)_P D_{\bar{B}}\bar{c}_0}{(\rho C)_f}, N_t = \frac{(\rho C)_P D_T\bar{T}_0}{(\rho C)_f\beta}, G_r = \frac{g\beta\bar{T}_0 R_0^3}{\gamma^2}, B_r = \frac{g\beta\bar{C}_0 R_0^3}{\gamma^2}, \bar{F} = \frac{F}{\mu W\ \lambda}, \theta_t = \frac{T - \overline{T_0}}{\overline{T_0}}\\
&\sigma = \frac{C - \overline{C_0}}{\overline{C_0}}, M = \frac{\sigma R_0^2 B_0^2}{\rho v}
\end{aligned} \tag{9}$$

The equations Eq. (2) to (8) becomes

$$\frac{\partial w}{\partial r} + \frac{w}{r} + \frac{\partial w}{\partial z} = 0 \tag{10}$$

$$\frac{\partial P}{\partial r} = -\frac{cos\alpha}{F} \tag{11}$$

$$\frac{\partial P}{\partial z} - \frac{sin\alpha}{F} = \frac{1}{r}\frac{\partial}{\partial r}\left(r\frac{\partial w}{\partial r}\right) + G_r\theta_t + B_r\sigma - \frac{\mu w}{k} - \sigma {B_0}^2 w \tag{12}$$

$$\frac{1}{r}\frac{\partial}{\partial r}\left(r\frac{\partial \theta_t}{\partial r}\right) + N_b\frac{\partial \sigma}{\partial r}\frac{\partial \theta_t}{\partial r} + N_t\left(\frac{\partial \theta_t}{\partial r}\right)^2 = 0 \tag{13}$$

$$\frac{1}{r}\frac{\partial}{\partial r}\left(r\frac{\partial \sigma}{\partial r}\right) + \frac{N_t}{N_b}\left(\frac{1}{r}\frac{\partial}{\partial r}\left(r\frac{\partial \theta_t}{\partial r}\right)\right) = 0 \tag{14}$$

Here, w is velocity with radius R_0. And, N_b, N_t are respectively Brownian motion parameter and Thermophoresis parameter. G_r, B_r being local temperature Grashof number and local nanoparticle Grashof number. θ_t, σ denotes temperature profile and nanoparticle phenomena respectively. Also, k is porous medium permeability, μ is viscosity of fluid and $M = \sigma {B_0}^2$ is magnetic parameter.

Non-dimensional boundary conditions are

$$\begin{aligned} &\frac{\partial w}{\partial r} = 0, \frac{\partial \theta_t}{\partial r} = 0, \frac{\partial \sigma}{\partial r} = 0 \text{ at } r = 0 \\ &w = 0, \theta_t = 0, \sigma = 0 \text{ at } r = R(z) \\ &w \text{ is finite at } r = 0 \end{aligned} \tag{15}$$

3 Solution

The coupled Equations (13) and (14) solutions are obtained by using (HPM), given below

$$H(q_t, \theta_t) = (1 - q_t)\left[L(\theta_t) - L(\theta_{10})\right] + q_t\left[L(\theta_t) + N_b\frac{\partial \sigma}{\partial r}\frac{\partial \theta_t}{\partial r} + N_t\left(\frac{\partial \theta_t}{\partial r}\right)^2\right] \tag{16}$$

$$H(q_t, \sigma) = (1 - q_t)\left[L(\sigma) - L(\sigma_{10})\right] + q_t\left[L(\sigma) + \frac{N_t}{N_b}\left(\frac{1}{r}\frac{\partial}{\partial r}\left(r\frac{\partial \theta_t}{\partial r}\right)\right)\right] \tag{17}$$

Here q_t is embedding parameter, lies between 0 and 1. $L \equiv \frac{1}{r}\frac{\partial}{\partial r}\left(r\frac{\partial}{\partial r}\right)$ is Linear operator. The initial guesses θ_{10} and σ_{10} are

$$\theta_{10}(r, z) = \left(\frac{r^2 - h^2}{4}\right), \quad \sigma_{10}(r, z) = -\left(\frac{r^2 - h^2}{4}\right) \tag{18}$$

$$\theta_t(r, z) = \theta_{t_0} + q_t\theta_{t_1} + q_t^2\theta_{t_2} + \ldots \tag{19}$$

$$\sigma(r, z) = \sigma_0 + q_t\sigma_1 + q_t^2\sigma_2 + \ldots \tag{20}$$

The series (19) and (20) in many cases are convergent. This convergent is based on the expression's Non-linear part. For $q_t = 1$,

$$\theta_t(r, z) = \left(\frac{r^2 - h^2}{64}\right)(N_b - N_t) \tag{21}$$

$$\sigma(r, z) = -\left(\frac{r^2 - h^2}{4}\right)\frac{N_t}{N_b} \tag{22}$$

Substituting equations (21) and (22) in (12) and by taking boundary conditions, the solution of the velocity is

$$w(r,z)=\frac{1}{\left[1-\frac{r^2}{4}\left(\frac{\mu}{k}+\sigma B_0^2\right)\right]}\left[\left(\frac{r^2-h^2}{4}\right)\left(-\frac{\sin\alpha}{F}+\frac{dP}{dz}\right)+B_r\frac{N_t}{N_b}\left(\frac{r^4}{64}-\frac{r^2h^2}{16}+\frac{3h^4}{64}\right)-G_r(N_b-N_t)\left(\frac{r^6}{2304}-\frac{r^2h^4}{256}+\frac{h^6}{288}\right)\right] \quad (23)$$

$$The\ dimension\ less\ flux\ is\ q=\int_0^h 2rwdr \quad (24)$$

The flux obtained by substituting (23) in (24) is

$$q=\left(\frac{h^4}{8}+\left(\frac{\mu}{k}+\sigma {B_0}^2\right)\frac{h^6}{96}\right)\left(\frac{sin\alpha}{F}-\frac{dP}{dz}\right)+B_r\frac{N_t}{N_b}\left(\frac{h^6}{48}+\frac{5h^8}{3072}\left(\frac{\mu}{k}+\sigma {B_0}^2\right)\right)-G_r(N_b-N_t)\left(\frac{5h^8}{3072}+\frac{h^{10}}{7680}\left(\frac{\mu}{k}+\sigma {B_0}^2\right)\right) \quad (25)$$

$$\Rightarrow\frac{dP}{dz}=\frac{1}{\left(\frac{h^4}{8}+\frac{h^6}{96}\left(\frac{\mu}{k}+\sigma B_0^2\right)\right)}\left[-q+\left(\frac{h^4}{8}+\frac{h^6}{96}\left(\frac{\mu}{k}+\sigma B_0^2\right)\right)\frac{\sin\alpha}{F}-G_r(N_b-N_t)\left(\frac{5h^8}{3072}+\frac{h^{10}}{7680}\left(\frac{\mu}{k}+\sigma B_0^2\right)\right)+B_r\frac{N_t}{N_b}\left(\frac{h^6}{48}+\frac{5h^8}{3072}\left(\frac{\mu}{k}+\sigma B_0^2\right)\right)\right] \quad (26)$$

$\triangle p=p(0)-p(\lambda)$ is pressure drop per wave length, defined as $\triangle p=-\int_0^1\frac{dP}{dz}\,dz$

$$=\int_0^1\frac{1}{\left(\frac{h^4}{8}+\frac{h^6}{96}\left(\frac{\mu}{k}+\sigma B_0^2\right)\right)}\left[q-\left(\frac{h^4}{8}+\frac{h^6}{96}\left(\frac{\mu}{k}+\sigma B_0^2\right)\right)\frac{\sin\alpha}{F}+G_r(N_b-N_t)\left(\frac{5h^8}{3072}+\frac{h^{10}}{7680}\left(\frac{\mu}{k}+\sigma B_0^2\right)\right)-B_r\frac{N_t}{N_b}\left(\frac{h^6}{48}+\frac{5h^8}{3072}\left(\frac{\mu}{k}+\sigma B_0^2\right)\right)\right]dz \quad (27)$$

The flow resistance (or) flow impedance λ is given as $\lambda=\frac{\triangle p}{q}$

$$=\frac{1}{q}\int_0^1\frac{1}{\left(\frac{h^4}{8}+\frac{h^6}{96}\left(\frac{\mu}{k}+\sigma B_0^2\right)\right)}\left[q-\left(\frac{h^4}{8}+\frac{h^6}{96}\left(\frac{\mu}{k}+\sigma B_0^2\right)\right)\frac{\sin\alpha}{F}+G_r(N_b-N_t)\left(\frac{5h^8}{3072}+\frac{h^{10}}{7680}\left(\frac{\mu}{k}+\sigma B_0^2\right)\right)-B_r\frac{N_t}{N_b}\left(\frac{h^6}{48}+\frac{5h^8}{3072}\left(\frac{\mu}{k}+\sigma B_0^2\right)\right)\right]dz \quad (28)$$

In absence of stenosis $h=1$, pressure drop is represented as $\triangle p_n$ and is found from Equation (27) as

$$\Delta p_n=\int_0^1\frac{1}{\left(\frac{1}{8}+\frac{1}{96}\left(\frac{\mu}{k}+\sigma B_0^2\right)\right)}\left[q-\left(\frac{1}{8}+\frac{1}{96}\left(\frac{\mu}{k}+\sigma B_0^2\right)\right)\frac{\sin\alpha}{F}+G_r(N_b-N_t)\left(\frac{5}{3072}+\frac{1}{7680}\left(\frac{\mu}{k}+\sigma B_0^2\right)\right)-B_r\frac{N_t}{N_b}\left(\frac{1}{48}+\frac{5}{3072}\left(\frac{\mu}{k}+\sigma B_0^2\right)\right)\right]dz \quad (29)$$

The flow impedance in normal artery is

$$\lambda_n=\frac{\triangle p_n}{q}$$

$$= \frac{1}{q}\int_0^1 \frac{1}{\left(\frac{1}{8}+\frac{1}{96}\left(\frac{\mu}{k}+\sigma B_0^2\right)\right)}\left[q-\left(\frac{1}{8}+\frac{1}{96}\left(\frac{\mu}{k}+\sigma B_0^2\right)\right)\frac{\sin\alpha}{F}+G_r\left(N_b-N_t\right)\left(\frac{5}{3072}+\right.\right.$$
$$\left.\left.\frac{1}{7680}\left(\frac{\mu}{k}+\sigma B_0^2\right)\right)-B_r\frac{N_t}{N_b}\left(\frac{1}{48}+\frac{5}{3072}\left(\frac{\mu}{k}+\sigma B_0^2\right)\right)\right]dz \tag{30}$$

$$The\ normalized\ flow\ impedance\ is\ \bar{\lambda}=\frac{\lambda}{\lambda_n} \tag{31}$$

The wall shear stress is

$\tau_h = -\frac{h}{2}\frac{dP}{dz}$

$$= -\frac{h}{2}\left[\frac{1}{\left(\frac{h^4}{8}+\frac{h^6}{96}\left(\frac{\mu}{k}+\sigma B_0^2\right)\right)}\left[-q+\left(\frac{h^4}{8}+\frac{h^6}{96}\left(\frac{\mu}{k}+\sigma B_0^2\right)\right)\frac{\sin\alpha}{F}-G_r\left(N_b-N_t\right)\left(\frac{5h^8}{3072}+\right.\right.\right.$$
$$\left.\left.\left.\frac{h^{10}}{7680}\left(\frac{\mu}{k}+\sigma B_0^2\right)\right)+B_r\frac{N_t}{N_b}\left(\frac{h^6}{48}+\frac{5h^8}{3072}\left(\frac{\mu}{k}+\sigma B_0^2\right)\right)\right]\right] \tag{32}$$

4 Results and Discussion

The influence of various fluid stream parameters on flow impedance $\left(\bar{\lambda}\right)$, wall shear stress (τ_h) for three types of arterial forms (converging, non-tapered and diverging tapering artery) are studied.

The physical characteristics of the flow parameters on flow impedance $\left(\bar{\lambda}\right)$ are displayed in Figures 2, 3, 4, 5, 6, 7, 8 and 9 . Impedance to the flow is noted to increase with the increase of local nanoparticle Grashof number (B_r), Inclination (α) and Magnetic parameter (M), but decreases with Brownian motion parameter (N_b) and shape parameter (n).

It is interesting to note that, with the increase of local temperature Grashof number (G_r) and Thermophoresis parameter (N_t), impedance to the flow is also increasing. But there is no much significance upto $\delta = 0.04$ and observed a significant variation in the remaining part of the domain. Similarly, it is concluded that, with the increase of permeability constant (k), impedance to the flow is decreasing, and this impedance is very small in the region $0 < \delta < 0.06$. This is true for diverging tapering, non-tapered artery and converging tapering.

Effects of various flow parameters on shear stress (τ_h) are shown in Figures 10, 11, 12, 13, 14, 15, 16, 17, 18 and 19 . The observation noted that, the wall shear stress enhances with the rise of B_r, G_r, N_t and k, but decreases with N_b, n, M and viscosity of the fluid.

Figures 20 and 21 displays the temperature profile variation with N_t and N_b respectively. An increase in temperature profile is observed by enhancing N_t , while decreases by enhancing N_b.

Figures 22 and 23 shows the variation of nano particle phenomena with N_t and N_b respectively. It is observed that, nano particle phenomena increase with N_t, but decreases with N_b.

To discuss trapping phenomenon, streamlines are drawn to examine flow pattern in presence of various parameters. Figures 24 and 25 displays stream lines for different values of k and M. Figure 24 displays the streamlines for the permeability constant (k). It reveals that, as we rise (k), bolus area is decreasing and the amount of boluses rises. Figure 25 reveals the stream lines behaviour for Magnetic parameter, which shows that less boluses are found with the increased magnetic parameter and bolus area is also increasing.

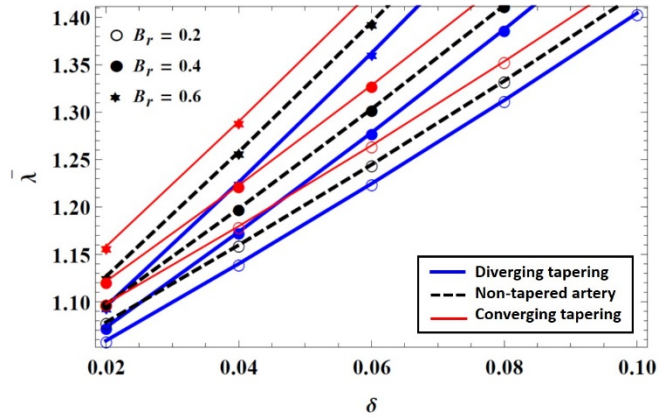

Fig 2. Effect of δ on $\bar{\lambda}$ with B_r varying

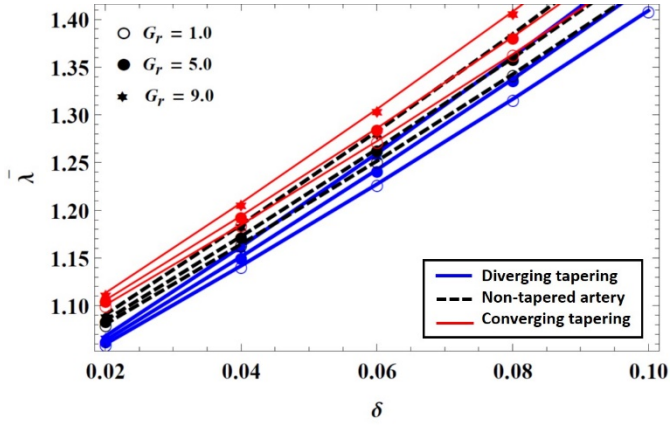

Fig 3. Effect of δ on $\bar{\lambda}$ with G_r varying

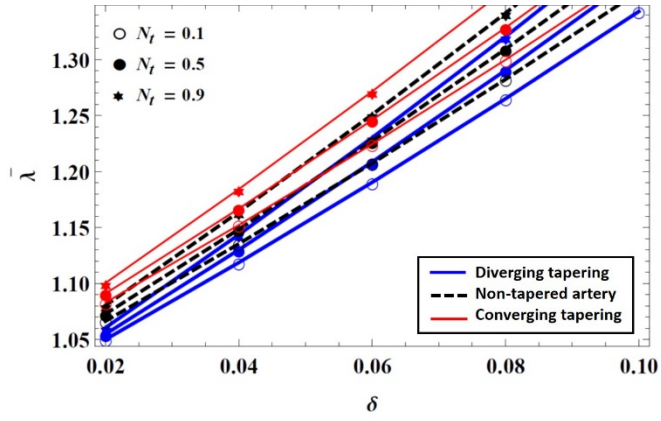

Fig 4. Effect of δ on $\bar{\lambda}$ with N_t varying

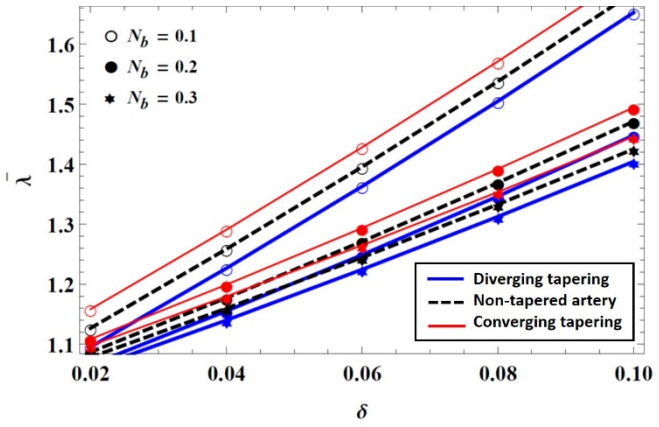

Fig 5. Effect ofδ on $\bar{\lambda}$ with N_b varying

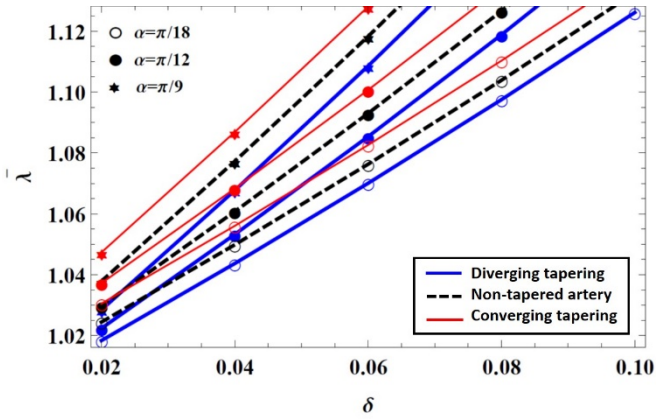

Fig 6. Effect of δ on $\bar{\lambda}$ with α varying

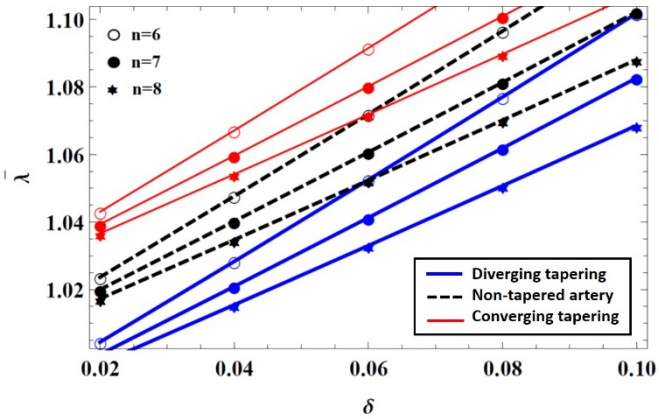

Fig 7. Effect ofδ on $\bar{\lambda}$ with n varying

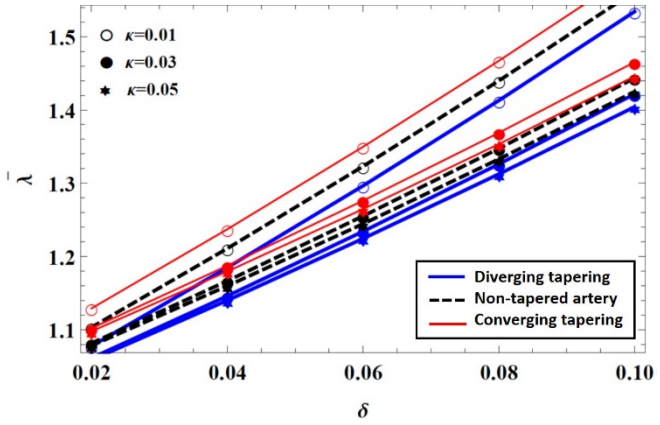

Fig 8. Effect of δ on $\bar{\lambda}$ with k varying

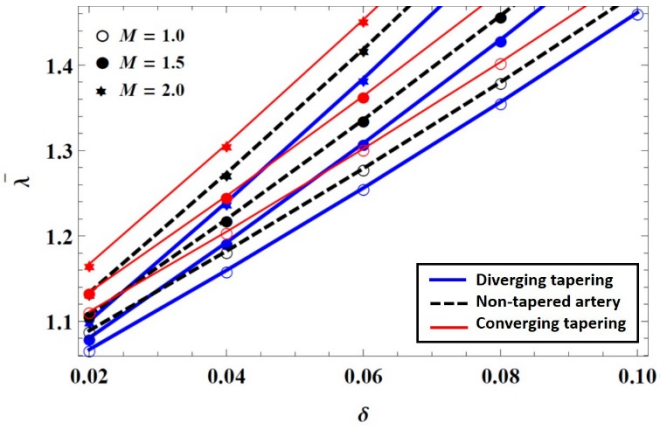

Fig 9. Effect of δ on $\bar{\lambda}$ with M varying

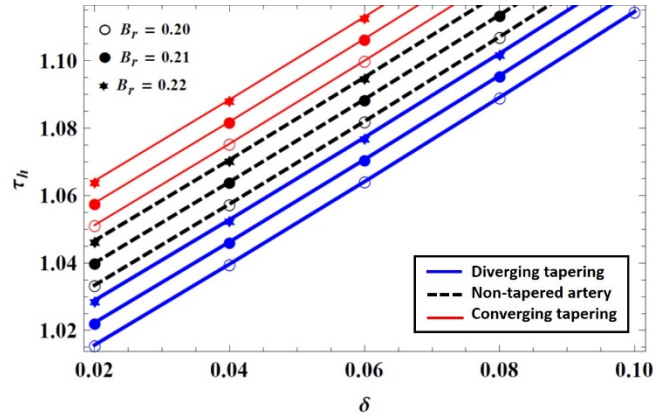

Fig 10. Effect of δ on τ_h with B_r varying

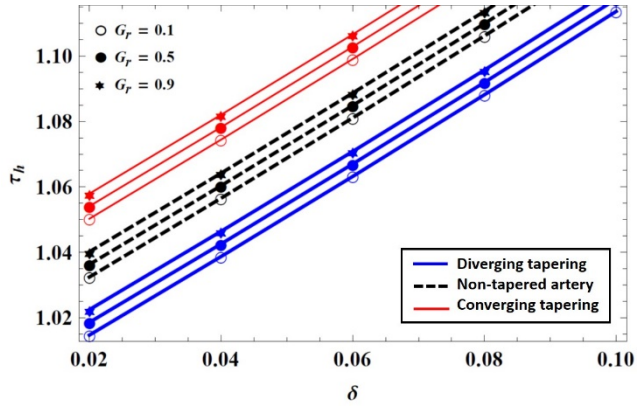

Fig 11. Effect of δ on τ_h with G_r varying

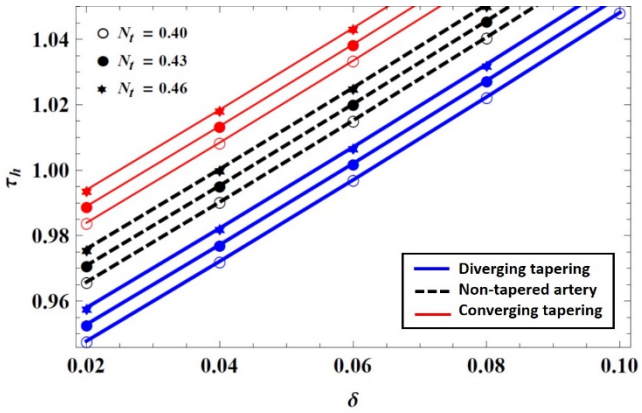

Fig 12. Effect of δ on τ_h with N_t varying

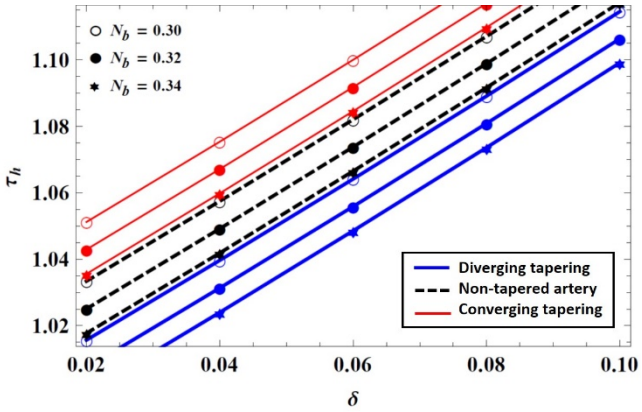

Fig 13. Effect of δ on τ_h with N_b varying

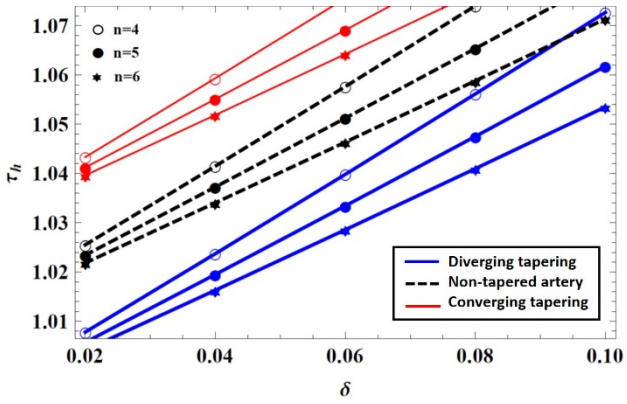

Fig 14. Effect ofδ on τ_h with n varying

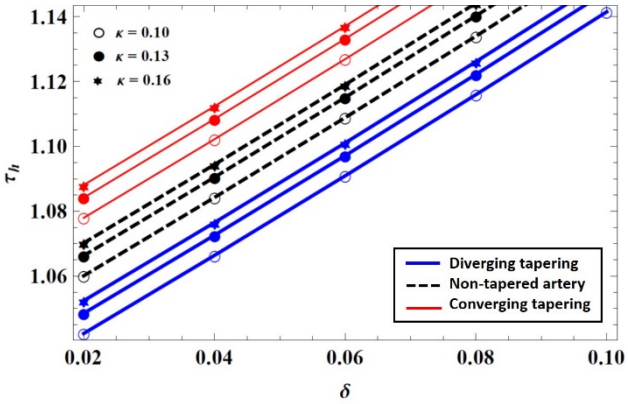

Fig 15. Effect of δ on τ_h with k varying

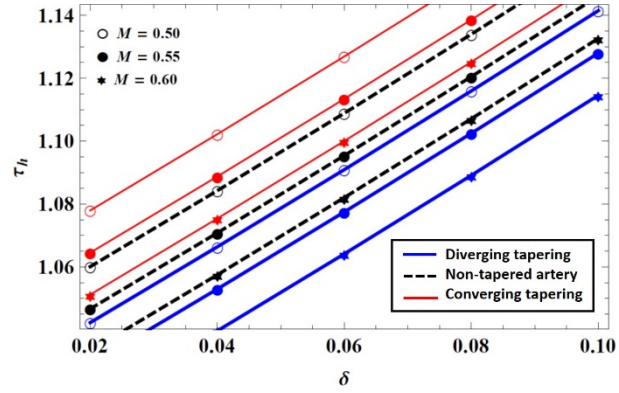

Fig 16. Effect ofδ on τ_h with M varying

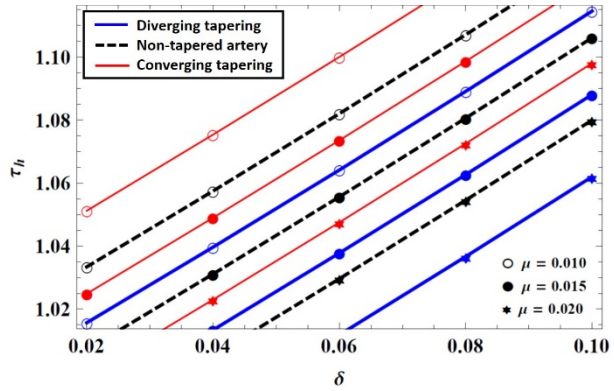

Fig 17. Effect of δ on τ_h with μ varying

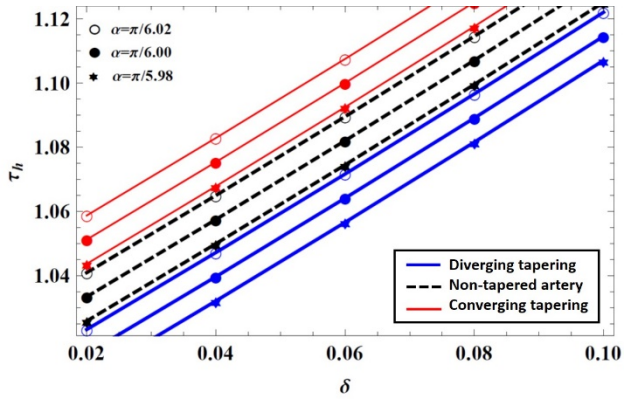

Fig 18. Effect of δ on τ_h with α varying

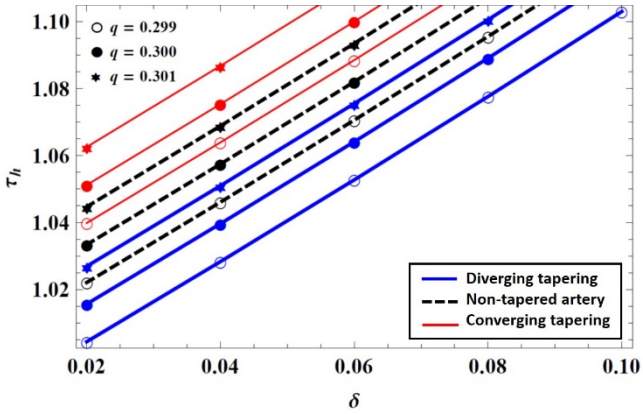

Fig 19. Effect of δ on τ_h with q varying

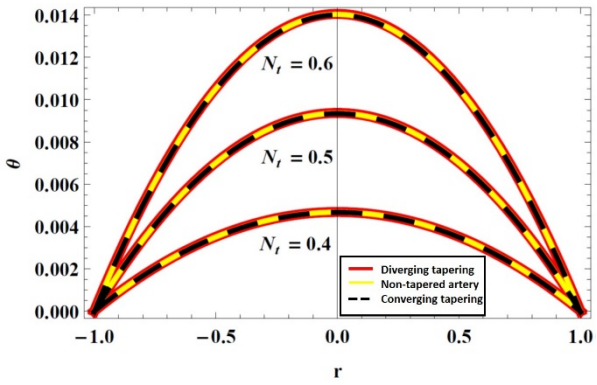

Fig 20. Variation in θ with N_t varying

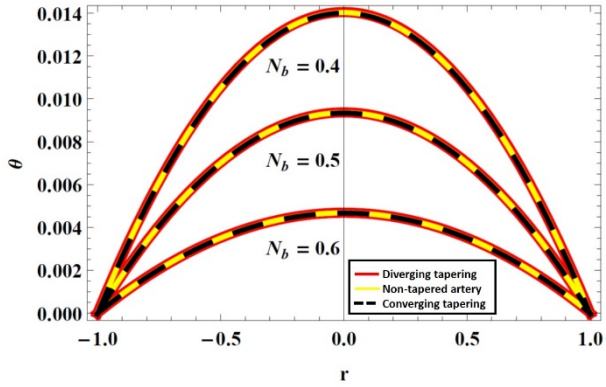

Fig 21. Variation in θ with N_b varying

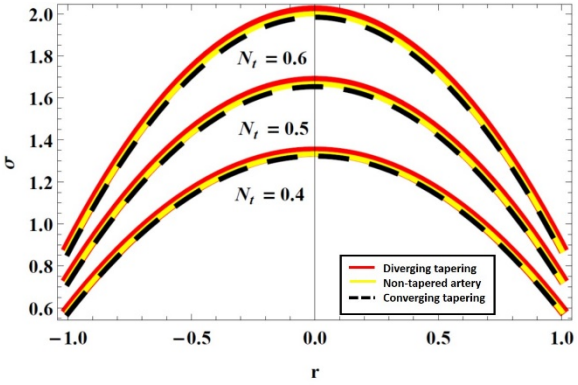

Fig 22. Variation in σ with N_t varying

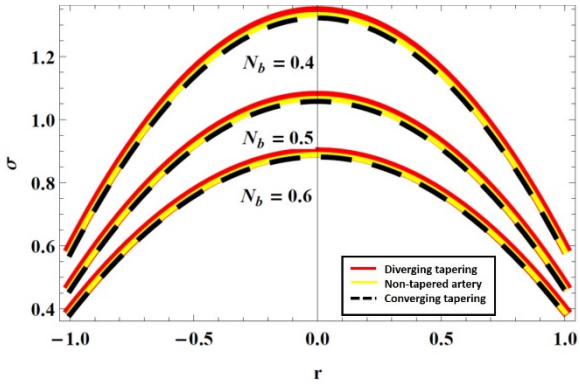

Fig 23. Variation in σ with N_b varying

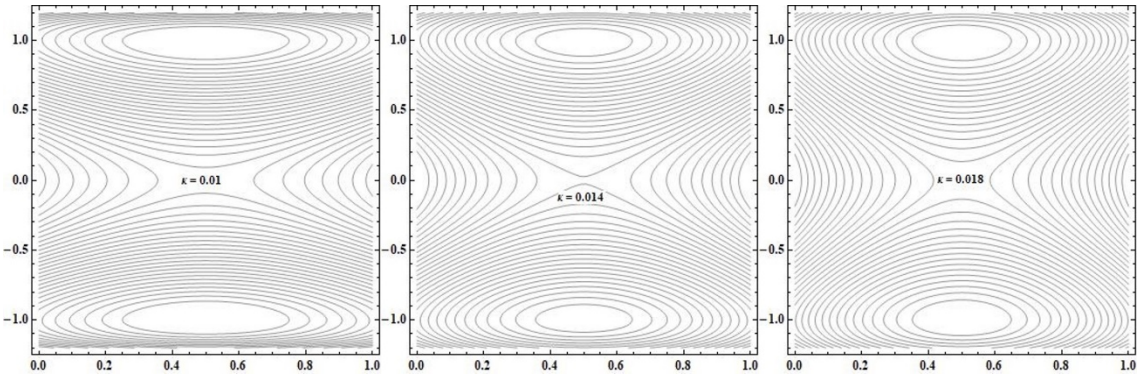

Fig 24. Stream line patterns for $k = 0.01,\ 0.014,\ 0.018$

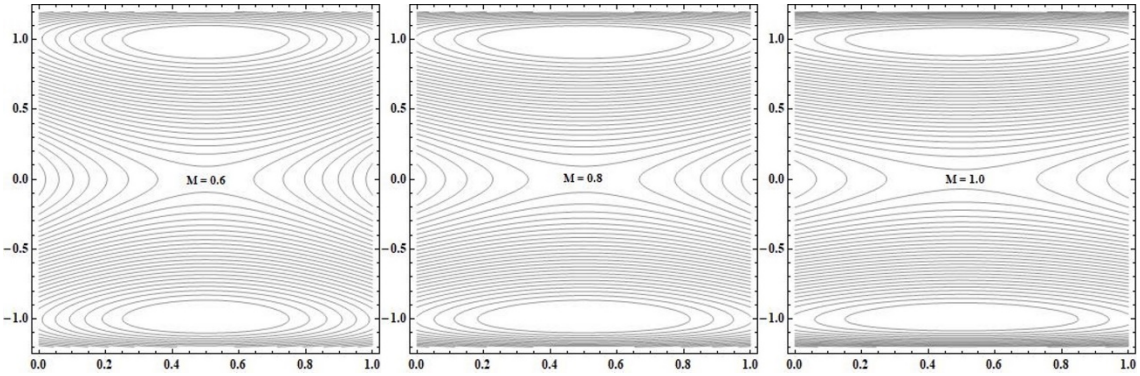

Fig 25. Stream line patterns for $M = 0.6,\ 0.8,\ 1.0$

5 Conclusion

Under the magnetic effect, the influence of various parameters on blood flow having nano fluid particles in an inclined tapering artery across permeable walls is studied.

The conclusions of this model are

1. It is identified that, impedance to the flow is getting higher for flow parameters like B_r, G_r, α and Magnetic parameter(M) respectively for diverging, non-tapered and converging tapering. Also, the impedance to the flow decreases with increase of n and volumetric flow rate(q).
2. The velocity of the particles with the surrounding molecules (N_t) is seen to increase with the stenosis height.

3. It is important to note that, with the increase of collision between the molecules, the flow resistance decreases. I.e., Brownian motion parameter (N_b).
4. It is remarkable to note that, the flow impedance decreases with the increase of the permeability (k) .
5. The observation noted that wall shear stress enhances with rise of B_r, G_r, N_t and k, but decreases with N_b, n, M, μ and volumetric flow rate (q).
6. Temperature profile increases by increasing (N_t) but decreases by increasing (N_b)
7. Nano particle phenomena increases by increasing (N_t) but decreases by increasing (N_b)
8. Amount of boluses are increasing as we enhance k, but the area of bolus is reducing.
9. With increase of Magnetic parameter, bolus area is broadening and amount of bolus are decreasing.

References

1) Padmanabhan N. Mathematical model of arterial stenosis. *Medical & Biological Engineering & Computing*. 1980;18(3):281–286. Available from: https://dx.doi.org/10.1007/bf02443380.
2) Shukla JB, Parihar RS, Rao BR. Effects of stenosis on non-Newtonian flow of the blood in an artery. *Bulletin of Mathematical Biology*. 1980;42(3):283–294. Available from: https://doi.org/10.1007/BF02460787.
3) Roy R, Riahi DN, Carrasquero N. Mathematical modeling of blood flow in an artery with an unsteady stenosis using power-law fluid model. .
4) Prasad KM, Yasa PR. Flow of non-Newtonian fluid through a permeable artery having non-uniform cross section with multiple stenosis. *Journal of Naval Architecture and Marine Engineering*. 2020;17:31–38. Available from: https://dx.doi.org/10.3329/jname.v17i1.40942.
5) Choi SU, Eastman JA. Enhancing thermal conductivity of fluids with nanoparticles. Argonne National Lab., IL (United States). 1995.
6) Prasad KM, Yasa PR. Mathematical Modelling of an Electrically conducting Fluid flow in an Inclined Permeable Tube with Multiple Stenoses. *International Journal of Innovative Technology and Exploring Engineering*. 2019;9(1):3915–3921.
7) Sinha A, Misra JC. Influence of Slip Velocity on blood flow through an artery with Permeable Wall: A Theoretical Study. *International Journal of Biomathematics*. 2012;05(05). Available from: https://dx.doi.org/10.1142/s1793524511001842.
8) Akbar NS, Rahman SU, Ellahi R, Nadeem S. Nano fluid flow in tapering stenosed arteries with permeable walls. *International Journal of Thermal Sciences*. 2014;85:54–61. Available from: https://dx.doi.org/10.1016/j.ijthermalsci.2014.06.009.
9) Crawford FW, Hoover GM. Flow of fluids through porous mediums. *Journal of Geophysical Research*. 1966;71(12):2911–2917. Available from: https://dx.doi.org/10.1029/jz071i012p02911.
10) Kasaeian A, Daneshazarian R, Mahian O, Kolsi L, Chamkha AJ, Wongwises S, et al. Nanofluid flow and heat transfer in porous media: A review of the latest developments. *International Journal of Heat and Mass Transfer*. 2017;107:778–791. Available from: https://dx.doi.org/10.1016/j.ijheatmasstransfer.2016.11.074.
11) Ramamurthy G, Shanker B. Magnetohydrodynamic effects on blood flow through a porous channel. *Medical & Biological Engineering & Computing*. 1994;32(6):655–659. Available from: https://dx.doi.org/10.1007/bf02524242.
12) El-Shehawey EF, Husseny SZA. Peristaltic transport of a magneto-fluid with porous boundaries. *Applied Mathematics and Computation*. 2002;129(2-3):421–440. Available from: https://dx.doi.org/10.1016/s0096-3003(01)00054-6.
13) Mandal PK. An unsteady analysis of non-Newtonian blood flow through tapered arteries with a stenosis. *International Journal of Non-Linear Mechanics*. 2005;40(1):151–164. Available from: https://doi.org/10.1016/j.ijnonlinmec.2004.07.007.
14) Tzirtzilakis EE. A mathematical model for blood flow in magnetic field. *Physics of Fluids*. 2005;17(7). Available from: https://dx.doi.org/10.1063/1.1978807.
15) Eldesoky IM. Slip effects on the unsteady MHD pulsatile blood flow through porous medium in an Artery under the effect of body acceleration. *International Journal of Mathematics and Mathematical Sciences*. 2012;2012:1–26. Available from: https://dx.doi.org/10.1155/2012/860239.